IMMUNOGLOBULIN SURFACE-BINDING KINETICS STUDIED BY TOTAL INTERNAL REFLECTION WITH FLUORESCENCE CORRELATION SPECTROSCOPY

NANCY L. THOMPSON AND DANIEL AXELROD
Department of Physics and Biophysics Research Division, University of Michigan, Ann Arbor, Michigan 48109

ABSTRACT An experimental application of total internal reflection with fluorescence correlation spectroscopy (TIR/FCS) is presented. TIR/FCS is a new technique for measuring the binding and unbinding rates and surface diffusion coefficient of fluorescent-labeled solute molecules in equilibrium at a surface. A laser beam totally internally reflects at the solid-liquid interface, selectively exciting surface-adsorbed molecules. Fluorescence collected by a microscope from a small, well-defined surface area $\sim 5\ \mu m^2$ spontaneously fluctuates as solute molecules randomly bind to, unbind from, and/or diffuse along the surface in chemical equilibrium. The fluorescence is detected by a photomultiplier and autocorrelated on-line by a minicomputer. The shape of the autocorrelation function depends on the bulk and surface diffusion coefficients, the binding rate constants, and the shape of the illuminated and observed region. The normalized amplitude of the autocorrelation function depends on the average number of molecules bound within the observed area. TIR/FCS requires no spectroscopic or thermodynamic change between dissociated and complexed states and no extrinsic perturbation from equilibrium. Using TIR/FCS, we determine that rhodamine-labeled immunoglobulin and insulin each nonspecifically adsorb to serum albumin-coated fused silica with both reversible and irreversible components. The characteristic time of the most rapidly reversible component measured is ~ 5 ms and is limited by the rate of bulk diffusion. Rhodamine-labeled bivalent antibodies to dinitrophenyl (DNP) bind to DNP-coated fused silica virtually irreversibly. Univalent F_{ab} fragments of these same antibodies appear to specifically bind to DNP-coated fused silica, accompanied by a large amount of nonspecific binding. TIR/FCS is shown to be a feasible technique for measuring absorption/desorption kinetic rates at equilibrium. In suitable systems where nonspecific binding is low, TIR/FCS should prove useful for measuring specific solute-surface kinetic rates.

INTRODUCTION

Association/dissociation reactions between biological molecules in solution and sites on a surface are involved in many important processes. When blood encounters a foreign surface, serum proteins adsorb, affecting subsequent interactions of biological molecules (Vroman and Adams, 1971; Brash and Lyman, 1971; Macritchie, 1978) and cells (Horbett and Weathersby, 1981; Grinnell and Feld, 1982; Neumann et al., 1979; Lahav et al., 1982) with the surface. For medical applications, substrate-immobilized antigens can be used to detect specific antibodies in a patient's serum (Giaver, 1978; Weetal, 1972). In industry, the manufacture and purification of biochemical products for medicine and biological research can use immobilized enzymes acting on substrates in solution (Mosbach, 1976; Lartigue and Yaverbaum, 1976). In cellular biology, hormones and neurotransmitters stimulate response by binding to specific receptors embedded in the plasma membrane of their target cells (Cuatrecasas, 1975; Whittaker, 1975; Kahn, 1976). Similarly, an immune response is triggered after viruses or antigens attach to immunological cells (Eisen, 1974; Clark, 1980).

Aside from its prominence in biology, medicine, and industry, the association/dissociation process itself holds theoretical interest. Nonspecific adsorption of solute molecules followed by surface diffusion can, under certain conditions, enhance reaction rates with specific sites on a surface (Adam and Delbrück, 1968; Berg and Purcell, 1977). Data gathered on model biochemical systems (Roberts and Hess, 1977; Wong et al., 1978) indirectly suggest that such rate enhancement indeed occurs in living systems.

We describe the application of a technique for directly measuring rate parameters critical to the association/dissociation process at a planar target, called total internal reflection with fluorescence correlation spectroscopy (TIR/FCS; Thompson, 1982 *a*). The theoretical and conceptual basis of TIR/FCS has previously been described (Thompson et al., 1981; Thompson, 1982 *b*). In TIR/FCS, fluorescent-labeled molecules are in chemical and thermodynamic equilibrium between a solution and a surface to

N. Thompson's present address is the Department of Chemistry, Stanford University, Stanford, CA 94305.

which they reversibly adsorb. A laser beam totally internally reflects at the surface-solution interface, forming an electromagnetic field called the "evanescent wave" in a very thin layer of solution immediately adjacent to the surface. Those fluorescent solute molecules that are adsorbed to the surface are selectively excited by the evanescent wave. A microscope collects the fluorescence arising from a small surface area, defined by an image plane aperture, and a photomultiplier measures the fluorescence intensity in time. As individual molecules bind and unbind within the observation area, or diffuse along the surface through it, the measured fluorescence fluctuates. The average rate of decay of the fluctuations, measured by minicomputer autocorrelation of the photmultiplier output, depends on the rates of association, dissociation, and surface diffusion.

FCS without internal reflection has been proposed for or applied to the measurement of diffusion coefficients and chemical reaction rates in solution (Elson and Magde, 1974; Magde et al., 1974; Phillies, 1975; Koppel, et al., 1976, Rigler et al., 1979; Borejdo, 1979), molecular weights (Weissman et al., 1976), rotational diffusion coefficients (Aragon and Pecora, 1976; Ehrenberg and Rigler, 1976; Yardley and Specht, 1976), laminar flow rates (Magde et al., 1978), diffusion in lipid bilayers (Fahey et al., 1976; Fahey and Webb, 1978; Dragsten and Webb, 1978), specific immunoglobulin concentration (Nicoli et al., 1980), and the radius of focused laser beams (Sorscher and Klein, 1980). FCS has also found applications in cell biology, to study motions of muscle cross-bridges during contraction (Borejdo et al., 1979), binding of ethidium bromide to DNA in the cell nucleus (Sorscher et al., 1980), and microaggregation of surface receptors (Peterson et al., 1981). Expressions for the statistical accuracy of FCS autocorrelation functions have been derived (Koppel, 1974). FCS has been combined with internal reflection to detect viruses in biological fluids (Hirschfeld et al., 1977).

Fluorescence excitation by total internal reflection (TIRF) has been used to study solutions of fluorescein (Hirschfeld, 1965), serum protein adsorption to solid surfaces (Watkins and Robertson, 1977; Harrick and Loeb, 1973; Lok et al., 1983 *a*; Lok et al., 1983 *b*), antibody binding to immobilized antigen (Kronick and Little, 1975; Kronick, 1974), and cell-substrate contact regions (Axelrod, 1981; Axelrod et al., 1983; Weis et al., 1982). Recently, TIRF has been combined with the fluorescence photobleaching recovery technique (Axelrod et al., 1976) to measure the adsorption kinetics and surface diffusion of serum albumin at glass (TIR/FPR; Thompson et al., 1981; Burghardt and Axelrod, 1981). TIRF has also been combined with singlet–singlet energy transfer methods to detect conformational changes of serum albumin upon adsorption to glass (Burghardt and Axelrod, 1983), and with anisotropy measurements to study the rotational diffusion of adsorbed fluorophores (Burghardt, 1983).

We apply TIR/FCS to the nonspecific reversible adsorption of rhodamine-labeled immunoglobulin molecules (R-IgG) to fused silica coated with irreversibly adsorbed bovine serum albumin (BSA-glass). This system was chosen as a first test of TIR/FCS both because of its ease of preparation and because of the importance of nonspecific binding of serum proteins in the interaction of molecular and cellular blood components with solid surfaces. As a test of the TIR/FCS technique on a different system, autocorrelation functions are also obtained from rhodamine-labeled insulin reversibly adsorbing to BSA-glass. These measurements are preliminary to the measurement of the binding kinetics of fluorescent-labeled hormones to biological or model cell surfaces and to surface-immobilized receptors.

A potential application of TIR/FCS is to the measure of specific binding kinetics between two chemical species, one of which is immobilized on a surface. We have attempted to measure binding rates of rhodamine-labeled mouse myeloma protein MOPC 315 (with known specificity for dinitrophenyl) or of its univalent hapten-binding fragments at a fused-silica surface coated with dinitrophenyl-conjugated BSA (DNP-BSA-glass). We find that nonspecific binding dominates specific binding at equilibrium unless the characteristic desorption time of specific binding is very long.

THEORY

When a light beam propagating through a transparent solid encounters an interface with a liquid, it undergoes internal reflection for oblique incidence angles (Harrick, 1967). An electromagnetic field, called the evanescent wave, penetrates into the liquid medium, and propagates parallel to the surface. The evanescent intensity decays exponentially with perpendicular distance from the surface, and at the surface is of the same order of magnitude of the incident light intensity for the incidence angles used in the TIR/FCS experiments. The characteristic $1/e$ depth d of the exponential intensity decay is

$$d = \frac{\lambda_o}{4\pi}(n_1^2 \sin^2\theta - n_2^2)^{-1/2}, \tag{1}$$

where λ_o is the light wavelength in vacuum, n_2 and n_1 are the refractive indicies of the liquid and the solid, and θ is the incidence angle measured from the perpendicular to the interface. Depth d decreases with increasing θ.

The derivation of the TIR/FCS autocorrelation function (Thompson et al., 1981; Thompson, 1982 *a*) uses a model in which molecules of bulk concentration $A(\mathbf{r},z,t)$ freely diffuse in solution and react with surface sites of concentration $B(\mathbf{r},t)$ to form fluorescent complexes of concentration $C(\mathbf{r},t)$. The reaction is represented by the chemical equation:

$$A(r,z,t) + B(r,t) \underset{k_2}{\overset{k_1}{\rightleftharpoons}} C(r,t). \tag{2}$$

Vector $\mathbf{r}$ is the position on the surface measured from the center of the observation area, z is the perpendicular distance from the surface to a point in solution, and t is the time. Parameters k_1 and k_2 are the on- and off-rate of the association/dissociation reaction at the surface, respectively, and K is the equilibrium constant, where

$$K = \langle C\rangle/\langle A\rangle\langle B\rangle = k_1/k_2, \tag{3}$$

and $\langle\ \rangle$ denotes thermodynamic ensemble average. Molecules diffuse in solution with coefficient D_A, and may diffuse along the surface with

coefficient D_C. A parameter β is defined as the average fraction of binding sites that remain free at equilibrium, and equals

$$\beta = \langle B \rangle / (\langle B \rangle + \langle C \rangle) = (1 + K\langle A \rangle)^{-1}. \quad (4)$$

The depth d is assumed to be very small compared with other characteristic distances in the system. Thus, each illuminated molecule is assumed to be bound to a surface site and not merely diffusing in bulk near the surface (see below). The measured fluorescence $F(t)$ is

$$F(t) = Q \int I_0 f(\mathbf{r})\, C(\mathbf{r},t)\, d^2r, \quad (5)$$

where Q is the product of the efficiencies of excitation light absorption and fluorescence emission and detection, I_0 is the maximum exciting light intensity, and the integration is taken over the plane of the liquid-solid interface. Function $f(\mathbf{r})$ is proportional to the product of the lateral profile formed by the totally internally reflected, focused laser beam (Burghardt, 1982) and the transmission function of the microscope's image plane aperture, and is a unitless function with unity maximum amplitude. The normalized autocorrelation function of fluorescence fluctuations, assuming a random, stationary signal, is:

$$G(\tau) = \langle \delta F(t+\tau)\delta F(t) \rangle / \langle F(t) \rangle^2 = \frac{\langle F(t+\tau)F(t) \rangle - \langle F(t) \rangle^2}{\langle F(t) \rangle^2}, \quad (6)$$

where $\delta F(t) = F(t) - \langle F(t) \rangle$ is the spontaneous fluctuation of fluorescence $F(t)$ at time t away from the mean fluorescence $\langle F(t) \rangle$.

When the observation area is very large, the parameters that determine the shape of $G(\tau)$ are a reaction rate R_R and a bulk diffusion rate R_B, where

$$R_R = k_2/\beta$$
$$R_B = D_A/(\beta\langle C \rangle / \langle A \rangle)^2. \quad (7)$$

The autocorrelation function $G(\tau)$ is equal to

$$G(\tau) = \frac{G(0)}{\upsilon_-^{1/2} - \upsilon_+^{1/2}} \cdot \{\upsilon_-^{1/2}\, w[-i(\upsilon_+ R_R \tau)^{1/2}] - \upsilon_+^{1/2}\, w[-i(\upsilon_- R_R \tau)^{1/2}]\}, \quad (8)$$

where

$$\upsilon_\pm^{1/2} \equiv 1/2(R_R/R_B)^{1/2}[-1 \pm (1 - 4R_B/R_R)^{1/2}],$$

and

$$w(i\eta) \equiv e^{\eta^2}\, erfc(\eta) \qquad (\eta \text{ complex}).$$

The value at time zero is (Thompson, 1982 *b*)

$$G(0) = \frac{1}{Z}\left[\frac{1}{\gamma(1-\beta)} - 1\right], \quad (9)$$

where Z is the total number of binding sites within the obervation area and γ is the fraction of molecules that are fluorescent labeled. $G(\tau)$ has simpler forms in the limiting cases of $R_B << R_R$ (bulk diffusion limit),[1] and $R_R << R_B$ (reaction limit):

$$G(\tau) \approx G(0) w(i\sqrt{R_B \tau}) \qquad (R_B \ll R_R)$$
$$G(\tau) \approx G(0) \exp(-R_R \tau) \qquad (R_R \ll R_B). \quad (10)$$

[1]Eq. 10 is incorrectly printed in Thompson et al., 1981, as $G(t) \simeq G(0)w(-i\sqrt{R_B\tau})$.

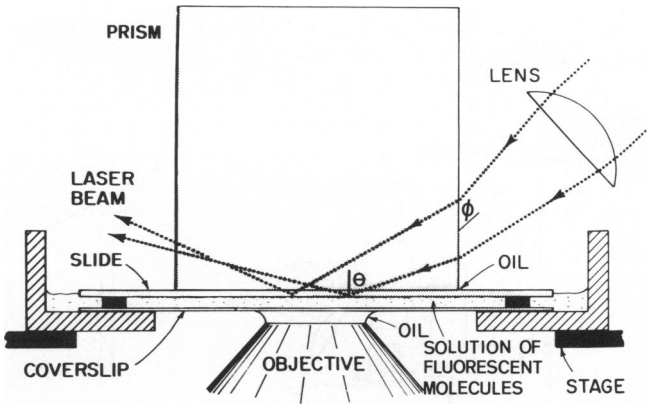

FIGURE 1 Optical apparatus. The laser beam is incident on a sample mounted on an inverted microscope. The beam either totally internally reflects at the sample (for TIR/FCS) or is focused with epi-illumination optics to a small spot in the sample (control experiments). Light collected by the objective passes through a filter to block scattered excitation light and (in some control experiments) the component of light polarized in a given direction. The filtered light is directed to an eyepiece, to a camera, or through an image plane aperture that defines a small surface observation area, to the photomultiplier. Fluctuations in the incident laser intensity are monitored by a photodiode.

MATERIALS AND METHODS

Optics

The optical apparatus of TIR/FCS is similar to that previously described for TIR/FPR (Burghardt and Axelrod, 1981). As depicted in Fig. 1, the beam of an argon ion laser (Lexel 95-3, Lexel Corp., Palo Alto, CA) is totally internally reflected at the solid-liquid interface of a BSA-coated fused-silica slide (1 in. × 1 in. × 1 mm) with a solution of the fluorescent protein. To achieve total internal reflection, the laser beam (λ_0 = 514.5 mm) is passed through a convex spherical focusing lens into a (1.5 cm)^3 cubic fused-silica prism (Precision Cells, Inc., Hicksville, NY). As shown in Fig. 2, the beam is incident on the vertical edge of the prism at an angle ϕ. The lower surface of the prism is in optical contact (via a thin layer of immersion oil) with the upper surface of the sample's fused-silica slide. Angle ϕ is large enough that the angle θ at which the beam is incident on the horizontal glass-solution interface is greater than the critical angle for total internal reflection. For fused silica (refractive index 1.46) and water (refractive index 1.33), the critical angle is $\sin^{-1}(1.33/1.46)$ = 65.6°, corresponding to a minimum ϕ of 53.0°.

The solution of fluorescent molecules is contained by a 35-mm diam plastic tissue-culture dish, ground to 1/8-in. height with a 1-in. hole drilled in the bottom and a No. 1 coverglass glued in with silicone cement. Two halves of an annular Teflon spacer of 1-in. outer diameter, 314-in. inner diameter and 0.0022-in. thickness (Nicholson Precision Instruments, Inc., Gaithersburg, MD) separate the slide from the bottom of the dish. The plastic dish is mounted in a brass plate that adapts to the stage of an inverted microscope (Leitz Diavert, E. Leitz, Inc., Rockleigh, NJ).

Fluorescence originating from the sample is collected by the microscope objective, passed through a filter to block scattered excitation light, and detected by a thermoelectrically cooled photomultiplier (RCA C31034A, RCA Electro-Optics & Devices, Lancaster, PA). The Teflon spacer is thin enough to permit use of high numerical aperture, short working distance objectives. Fluctuations in incident laser intensity (≤1%) are detected by a photodiode, and corrections for the fluctuations are made on-line while the data is autocorrelated, as in standard FCS (Koppel et al., 1976). The laser, microscope, and supporting optics are mounted on a vibration-isolated air table.

Fig. 3 shows fluorescence from a slide coated with an irreversibly

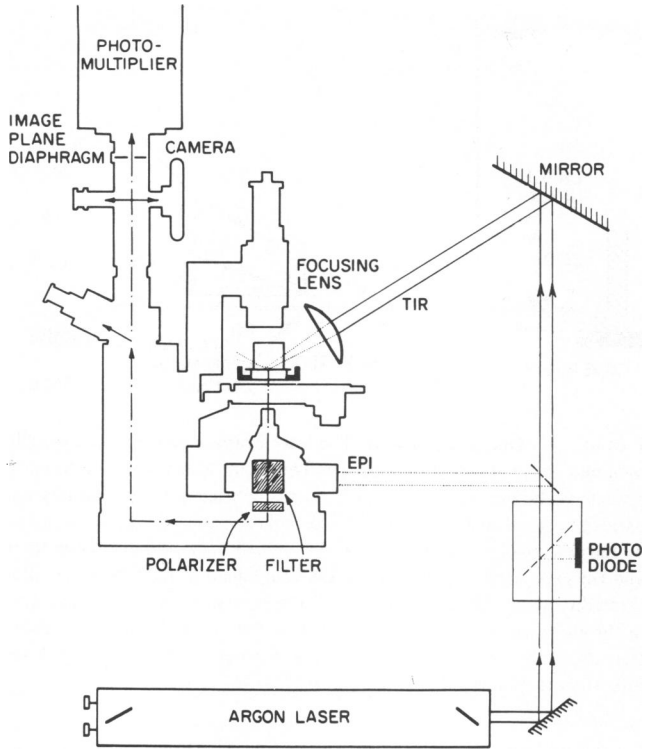

FIGURE 2 Sample holder. The laser beam, focused by a spherical convex lens, enters a cubic fused silica prism at angle ϕ. The prism is optically coupled with immersion oil to a fused-silica slide. The angle ϕ is large enough that the angle θ at which the beam is incident on the quartz-solution interface is greater than the critical angle. The beam totally internally reflects, illuminating fluorescent molecules that adsorb from the solution to the underside of the fused-silica slide. The solution is contained by a plastic tissue-culture dish where the bottom has been replaced by a glass coverslip and a thin spacer was inserted between the coverslip and slide. The sample is on the stage of an inverted microscope, and fluorescence arising from the surface is collected by a high numerical aperture objective.

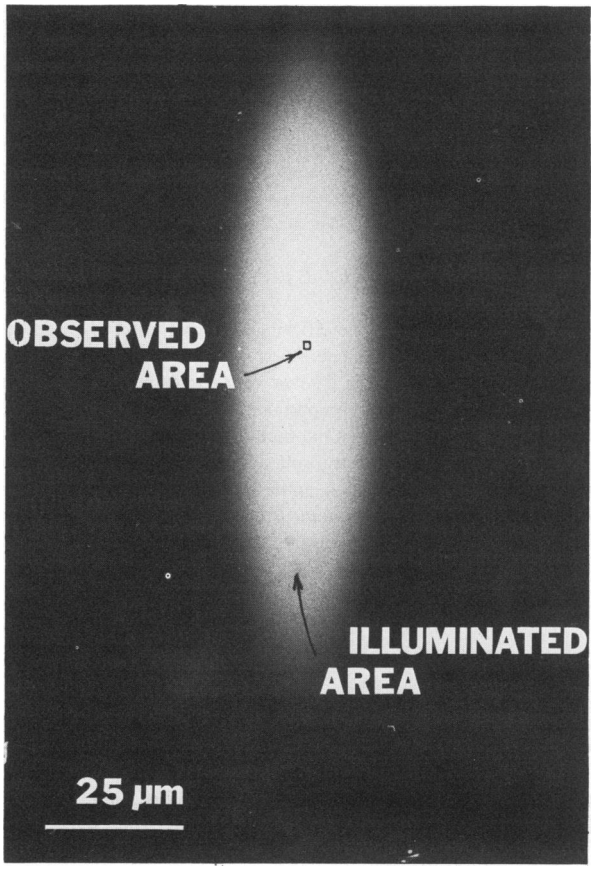

FIGURE 3 Lateral intensity profile of the evanescent wave. Pictured above is a photograph of the totally internally reflected laser beam exciting a fluorescent dye adhered to glass (courtesy of T. Burghardt). The intensity profile is of broad elliptical Gaussian shape. Only a small portion of the illuminated area, defined by the microscope's image plane aperture, is observed by the photomultiplier.

adsorbed fluorescent dye, 3, 3'-dioctadecylindocarbocyanine (diI), excited by the evanescent wave, and photographed through the microscope. As shown, the lateral intensity profile of the evanescent wave is elliptical. The area of the sample observed by the photomultiplier is much smaller than the area illuminated by the laser beam and is defined by a square aperture at a microscope image plane. At a magnification of 40, the aperture can be adjusted continuously to correspond to an area on the sample of $\sim(0.5\ \mu m)^2$ to $\sim(65\ \mu m)^2$, with an accuracy in each dimension of $\pm 0.1\ \mu m$.

Electronics

The output of the photmultiplier is sent through an amplifier/discriminator (Ortec Model 9302, EG & G Ortec, Oak Ridge, TN) to shape the photoelectron pulses and to filter low-level noise. A NOVA 3/12 minicomputer (Data General Corp., Westboro, MA), interfaced to the photon-detecting electronics, is used to autocorrelate the photon counts. The minicomputer interface counts the number of photoelectron pulses n_j occurring between consecutive sample times $j\Delta T$ to $(j + 1)\Delta T$. The sample time ΔT can be specified by the user and can range from 1 μs to $\sim$16 s. The n_j are counted as 16-bit binary words, stored in a first-in-first-out buffer, and transferred to the central processing unit. The interface also outputs the autocorrelation function in analog form (for oscilloscope display), as software increases the statistical accuracy of the autocorrelation function by using new n_j as they are counted. In addition, a separate output of the amplifier/discriminator is counted by a commerical photon counter (EG & G Ortec model 9315), converted to an analog signal (EG & G Ortec model 9325), and recorded on a strip chart (Heath-Schlumberger SR-206, Heath/Zenith, Heath Co., Benton Harbor, MI).

Autocorrelation Software

Using the n_j, the user-specified value of ΔT, and the user-specified total number of points P ($\leq$128 in our system) in the computed autocorrelation function, the software estimates $G(i\Delta T)$ as

$$G(i\Delta T) = \frac{\sum_{j=1}^{M} n_{(jm)}n_{(jm)-i} - n_{(jm)}n_{(jm)-k}}{\sum_{j=1}^{M} n_{(jm)}n_{(jm)-k}} (i = 0 \text{ to } P). \quad (11)$$

Subscript m is equal to unity for long sample times; it is larger than unity when ΔT is too short (<10 ms for a 128 point autocorrelation function) for the computer's rate of arithmetic calculation to match its rate of data acquisition. M is the number of terms summed during an experiment, with which both the estimation accuracy and the statistical accuracy of the autocorrelation function increase. Index k ranges from 1,152 to 1,279 and is much larger than the number of points P calculated in the autocorrelation function. It is given by $k = j + 1{,}152 - 128 \cdot J$, where J

is the greatest integer less than $(j-1)/128$. In effect, this procedure substitutes $\langle F(t)\rangle^2$ of Eq. 6 by $\lim_{\tau\to\infty} \langle F(t)F(t+\tau)\rangle$, a valid substitution for random signals. Index k, which varies as a function of j, averages over any periodic oscillations that may persist into the long time separation of data points. The products $n_{jm}n_{jm-i}$ and $n_{jm}n_{jm-k}$ are determined by an assembly language software add and shift left routine, or, for sufficiently low n_j, by a software multiplication table stored in memory.

Experimental Corrections to $G(\tau)$

If the value of fluorescence averaged over several seconds drifts slightly over the course of the autocorrelation (many minutes), then $G(i\Delta T)$, calculated according to Eq. 11, is offset from $G(\tau)$ given in Eq. 6. If the measured fluorescence $F(t)$ were a line of positive slope increasing from value F_1 to F_2 during the course of an experiment lasting for a time $T >> \Delta T$, then Eq. 11 implies that $G(i\Delta T)$ would be calculated as

$$G(i\Delta T) = 1{,}216\,\frac{(F_2 - F_1)}{F_2}\,\frac{\Delta T}{T}. \qquad (12)$$

The experimental functions in this paper have been corrected for this systematic error (always <10%).

In addition, for low fluorescent photon count rates, the background intensity may be a substantial portion of the signal. Background intensity arises from the photomultiplier dark count (~50 cps), some scattered room light, glass luminescence, and/or Raman scattering from the water. If the fluorescence due to molecular number fluctuations is $F(t)$ and the background is $F_0(t)$, then the autocorrelation function $G'(\tau)$ calculated by the minicomputer would be

$$G'(\tau) = \left[\frac{\langle F_0(t) + F(t)\rangle}{\langle F(t)\rangle}\right]^2 [G(\tau)], \qquad \tau > 0, \qquad (13)$$

where $G(\tau)$ is given by Eq. 6. The experimental autocorrelation functions in this paper have been multiplied by the inverse of the factor preceding $G(\tau)$ in Eq. 13 (never greater than 1.4).

Rhodamine-labeled Immunoglobulin for Nonspecific Binding Studies

Immunoglobulin molecules (IgG) were made optically fluorescent by reacting the isothiocyanate derivative of tetramethylrhodamine with the lysine residues of IgG (Amante et al., 1972). To 10 mg of lyophilized chromatographically purified rabbit IgG (82% protein, 18% phosphate and NaCl, Cappel Laboratories, Cochranville, PA) dissolved in 5 ml of 0.1 M $NaHCO_3$ pH 9.0 was added 59 μl of 1 mg/ml tetramethylrhodamine-isothiocyanate (TMR-ITC, BBL Microbiology Systems, Cockeysville, MD) in ethyl alcohol, so that the molar ratio of TMR-ITC to IgG was ~2. After incubating in the dark at room temperature for ~30 min, unreacted TMR-ITC was separated from IgG, and the pH was lowered by passing through a Sephadex G25-150 column in 0.1 M $NaPO_4$, 0.15 M NaCl, 0.02% NaN_3 pH 7.0 (PBS). The solutions were passed through a 0.22-μm pore Gelman filter and either used immediately, or stored either at 4°C (<4 d) or at −5°C. Solutions stored for >1 wk were rechromatographed and refiltered before use.

R-IgG Concentration and Degree of Labeling

The concentration of R-IgG and the average number of rhodamine groups conjugated to an IgG molecule (R/I) was calculated from the extinction coefficients of the rhodamine portion of R-IgG at 550 and 275 nm, the IgG portion of R-IgG at 275 nm [$\epsilon(R,550)$, $\epsilon(R,275)$, $\epsilon(I,275)$], and the optical densities of the samples at 275 and 550 nm. $\epsilon(I,275)$ was determined by measuring the optical density at 275 nm as a function of unlabeled IgG concentration (made fresh), and equals 182,000 $M^{-1}cm^{-1}$. The value of $\epsilon(R,550)$ was assumed to be 16,000 $M^{-1}cm^{-1}$ (Burghardt and Axelrod, 1981) and the value of $\epsilon(R,275)$ to be 13,000 $M^{-1}cm^{-1}$ (Burghardt, T. P., unpublished results). Using these values, we determined that the above protocol for rhodamine labeling yields molar values of R/I from 0.15 to 1.8. The exact degree of labeling varied from sample to sample.

Rhodamine-labeled Insulin

Bovine insulin (Sigma Chemical Co., St. Louis, MO) has one lysine residue, which was reacted with TMR-ITC according to the methods of Schechter et al. (1978). R-insulin in PBS was stored at −5°C and then purified on Sephadex G25-150 and passed through a 0.22 μm filter immediately before use.

Anti-DNP Preparations

Mineral oil–induced plasmacytoma 315 (MOPC 315; received as a gift from Anne Maddelena and Latham Claflin of the University of Michigan Hybridoma Facility, or purchased from Litton Bionetics, Inc., Kensington, MD) is a mouse myeloma IgA protein specific for the DNP group (Potter, 1972). MOPC 315, which occurs in several polymeric forms of a bivalent monomer, was treated for reduction to the pure monomer (Eisen et al., 1968; Underdown et al., 1971; Goetzl and Metzger, 1970). 1 ml of 1 mg/ml MOPC 315 was transferred to 0.2 M Tris pH 8.6 by chromatographing on a 10 ml Sephadex G25-150 column, and incubated with 0.01 M dithiothreitol (Sigma Chemical Co.) at room temperature for 1 h. A volume equal to that of the sample of 0.022 M iodoacetamide (Sigma Chemical Co.) in 0.2 M Tris pH 7.3 was added, the resultant solution was incubated at room temperature for 15 min, and the sample was dialyzed into PBS (for monomer experiments) or 0.1 M Tris 0.02 M $CaCl_2$ pH 8.0 (for F_{ab} experiments).

In F_{ab} experiments, the sample was incubated twice with 10 μl of 2 mg/ml TPCK-trypsin (Worthington Biochemicals Corp., Freehold, NJ) at 37°C for 3 h. The antibody solution was then dialyzed against 2 liters of 0.01 M Tris, 0.02% NaN_3 pH 7.3 for 8 h at 4°C, and then 2 liters of 0.01 M KPO_4, 0.05 M NaCl pH 7.9 overnight. F_{ab} fragments were isolated on a 10-ml Sephadex DEAE A-25 column packed in 0.01 M KPO_4, 0.05 M NaCl pH 7.9. The fragments were eluted (flow rate < 1 ml/min; fraction volume 1 ml) by applying 1 ml each of 0.01 M KPO_4 pH 7.9, 0.05 M, 0.075 M, ..., 0.275 M NaCl after the sample, followed by ~50 ml of 0.1 M KPO_4, 0.3 M NaCl, pH 7.9. The F_{ab} and F_c emerged as distinct peaks.

Control samples of tetramethylpentadecane-induced plasmacytoma (TEPC 15; Litton Bionetics) were prepared identically to MOPC 315 samples. TEPC 15 is a mouse myeloma protein that specifically binds to phosphorylcholine and not to DNP (Potter, 1972; Potter and Lieberman, 1970).

MOPC 315 and TEPC 15 (monomers and F_{ab}) were labeled with TMR-ITC (R-MOPC, R-TEPC) according to the protocol described above for IgG. The antibodies were labeled at R/I values of ~1. Antibody concentration is determined by the 280 nm optical density calibrated according to the Lowry (Lowry et al., 1951) and microbiuret (Janatova et al., 1968) methods of protein concentration determination. The calibration of rhodamine-labeled antibody changed by only 3% from that of unlabeled antibody. Unlabeled mouse IgG (Miles Laboratories, Inc., Elkhardt, IN) or TEPC 15 was added at 0.2–5.0 mg/ml to labeled antibody solutions.

When MOPC 315 binds to a DNP group, its 350 nm protein fluorescence is quenched (Eisen et al., 1968). To ensure that the F_{ab}-producing and rhodamine-labeling procedures in these experiments do not render the antibody inactive, the product of these preparations was tested for protein fluorescence quenching by DNP. Fig. 4 *a* shows the protein fluorescence (SLM Instruments, Inc. model 4000, Urbana-Champaign, IL) of R-MOPC F_{ab}, R-TEPC F_{ab}, mouse IgG, and PBS as a function of DNP-BSA concentration. When the molar amount of DNP-BSA added is approximately equal to that of R-MOPC F_{ab}, the fluorescence drops to 41% of its value in the absence of DNP-BSA. Under similar conditions, R-TEPC F_{ab} fluorescence drops only to 76% and mouse IgG to 75% of their initial values. In the absence of fluorescence

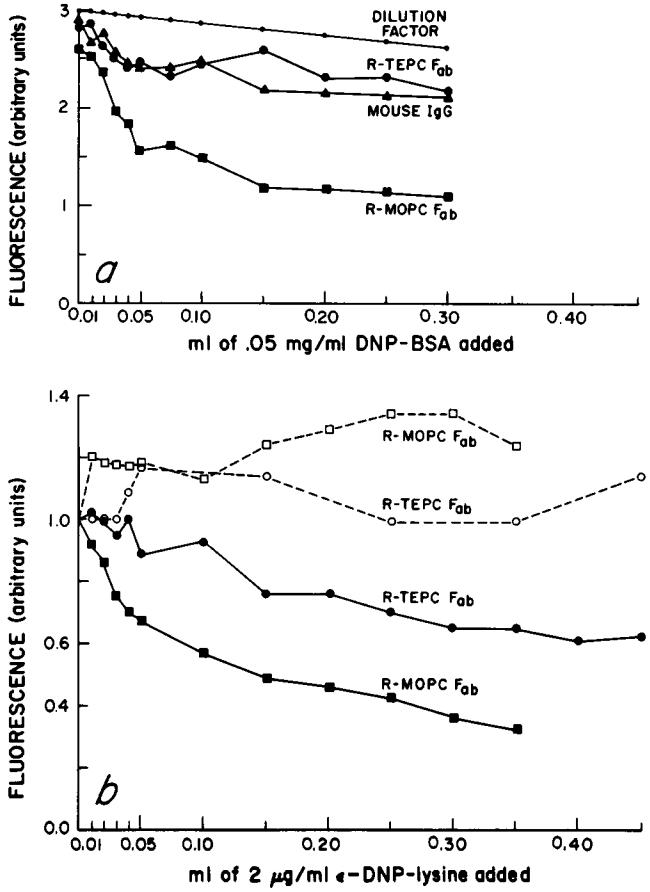

FIGURE 4 Fluorescence quenching of R-MOPC F_{ab} by DNP. (*a*) As DNP-BSA is added to 2 ml of 0.005 mg/ml solutions of R-MOPC F_{ab}, R-TEPC F_{ab}, mouse IgG, and PBS, protein fluorescence (excited at 280 nm and detected at 350 nm) is quenched more for R-MOPC F_{ab} than the other samples, demonstrating that the R-MOPC F_{ab} is active. The fluorescence of the DNP-BSA is negligible. The top curve shows the factor by which solutions are diluted with the addition of DNP-BSA solution. (*b*) As ε-DNP-lysine is added to 2 ml of 0.0035 mg/ml of R-MOPC F_{ab}, protein fluorescence (—) is quenched more for R-MOPC than R-TEPC, indicating that the R-MOPC is active. Rhodamine fluorescence (---) (excited at 550 nm and detected at 570 nm) is not quenched for either sample.

quenching, the protein fluorescence would decrease to 87% of the original value from dilution. Fig. 4 *b* shows similar results for R-MOPC F_{ab} and R-TEPC F_{ab} in the presence of ε-DNP-lysine (Sigma Chemical Co.). Fig. 4 *b* also shows the rhodamine fluorescence as a function of ε-DNP-lysine added, demonstrating that specifically bound DNP does not quench the fluorescence of rhodamine-labeled MOPC 315.

Albumin-coated Glass

Suprasil fused-silica 1 in. × 1 in. × 1 mm microscope slides (Amersil Inc., Hillside, NJ) were cleaned by first washing with soapy water and rinsing well with water. After a 1-h immersion in chromic acid, the slides were rinsed with 95% ethyl alcohol, distilled water, and spectrosopic grade acetone. The dry slides were placed in a Harrick PDC-3XG plasma cleaner (Harrick Scientific Corp., Ossining, NY) under argon gas on the high setting for 5–10 min. New and previously used slides were treated identically.

Lyophilized bovine serum albumin (BSA) or BSA conjugated with 30–40 DNP groups per molecule (DNP-BSA) (both from Calbiochem-Behring Corp., American Hoechst Corp., San Diego, CA) were dissolved in PBS at 3 mg/ml and passed through a 0.22 μm filter. Approximately 0.5 ml of the BSA or DNP-BSA solution was placed on top of a clean dry slide and the molecules were allowed to adsorb to the glass from the solution for at least 1 h. The slide was then rinsed quickly in 50 ml PBS and again in 50 ml PBS for 5 min to remove reversibly adsorbed BSA. After the second rinse, the slide was held vertically and touched to a tissue for a few seconds until most of the solution drained from the slide; it was immediately coated with fluorescent-labeled protein (IgG, insulin, or antibody), as described below. Control experiments in which the BSA or DNP-BSA was labeled with TMR-ITC, adsorbed to the glass, and observed under TIRF indicated that the albumin does indeed irreversibly adsorb to the slide.

Sample Preparation

PBS and then rhodamine-labeled protein solution were applied directly to a face-up albumin-coated slide. In nonspecific binding studies, the applied volume was always 0.2 ml. After a 15 min incubation, the albumin-coated slide with fluorescent protein solution on top was held horizontally above the dish (Fig. 2), tilted, and quickly flipped onto the Teflon spacers. The dish was mounted on the fluorescence microscope adapted for TIRF.

NONSPECIFIC BINDING RESULTS

Fluorescence vs. Excitation Light Intensity

The fluorescence of R-IgG adsorbed in equilibrium to BSA-glass does not increase linearly with exciting light intensity. This probably occurs because a multiplicity of R-IgG surface residency times are present, so that R-IgG bound irreversibly and with slow reversibility were photobleached under higher exciting light intensities. Consistent with this assumption, we observed an initial decay in fluorescence at the start of sample illumination. For the intensity used in these experiments (0.02 mW/μm^2), the measured fluorescence decays to 50% of its original value after several seconds, with a $1/e$-time of ~0.7 s. The average fluorescence then remains constant for at least 1 h of illumination. Autocorrelation is begun only after this pseudo–steady state is reached.

Fraction of Observed R-IgG Molecules That Are Surface Bound

To correctly interpret the TIR/FCS autocorrelation function, it is necessary to measure, under the same excitation intensity used for autocorrelation, the ratio of R-IgG in the observation area that are surface bound vs. freely diffusing in the bulk within the evanescent illumination. However, neither the R-IgG surface concentration nor bulk concentration (after depletion by adsorption to the surface of the sample chamber) are known a priori.

In principle, the fraction of illuminated R-IgG that are surface-bound can be determined from the ordinate intercept of a plot of measured fluorescence vs. evanescent field depth that can be varied with the incidence angle (Eq. 1). (This procedure assumes no change in the product of the extinction coefficient and quantum efficiency upon adsorption.) Another method of determining the surface-bound fraction of illuminated R-IgG would be to interpolate the

degree of polarization anisotropy of the sample's fluorescence, when excited with polarized light, between that of R-IgG irreversibly adsorbed and R-IgG in solution (Thompson, 1982 *a*). This approach utilizes the fact that fluorescence from rhodamine conjugated to BSA is less polarized in freely diffusing BSA than in irreversibly adsorbed BSA (Burghardt, T. P., 1983).

We have determined the equilibrium fraction of illuminated R-IgG that are surface-bound, by considering both the measured value of $G(0)$ and also the bulk concentration calibrated from the fluorescence excited in the bulk by epi-illumination. Following methods analogous to those of Thompson et al. (1981; Eqs. 23, 25, 47) for the case where fluorescence arises from both surface-adsorbed and bulk-dissolved fluorophores in an exponentially decaying evanescent field, one can show that

$$G(0) = \frac{\beta\langle N_C\rangle + \langle N_A\rangle/2}{(\langle N_C\rangle + \langle N_A\rangle)^2} \qquad (14)$$

where $\langle N_C\rangle = \langle C\rangle S$ is the number of surface bound molecules within an observation area S, and $\langle N_A\rangle = \langle A\rangle Sd$ is the number of freely diffusing molecules within the observation area. In addition, fluorescence calibration implies that an applied concentration of 0.033 mg/ml (typical in these experiments) is depleted, due to adsorption to the sample chamber, to 0.023 ± 0.005 mg/ml. Thus, for the autocorrelation function in Fig. 6 (R/I = 0.16, observation area 4.4 μm^2 and d = 0.1 μm), $\langle N_A\rangle$ is 6.5 ± 1.4. Using Eq. 14 with $G(0)$ = 0.019 ± 0.001 and β = 1 (see below), we then calculate that $\langle N_C\rangle$ equals 42.5 ± 3.4. The fraction of observed R-IgG molecules that are surface bound is thereby 0.87 ± 0.09, and the height of the autocorrelation function at time zero due to correlations in surface-bound molecular number fluctuations is 0.0176 ± 0.0021.

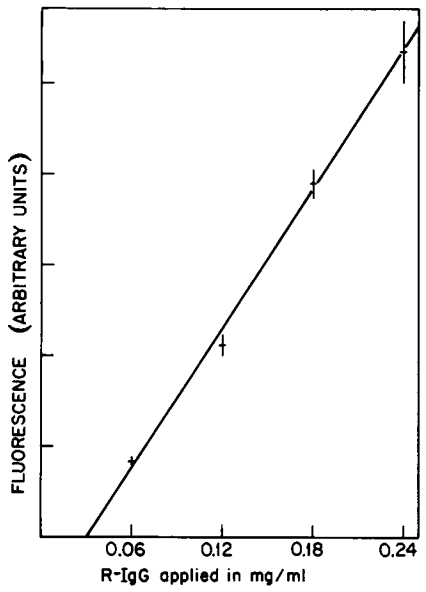

FIGURE 5 Fluorescence vs. bulk concentration. The surface fluorescence from R-IgG adsorbing to BSA-glass increases linearly with applied R-IgG bulk concentration. This indicates that the surface binding sites are far from saturated. Concentration values are those of a 0.2 ml R-IgG solution (R/I = 1.0) applied to the BSA-glass. Depletion due to adsorption to the bottom of sample holder (area ~5 cm^2) is not accounted for in these values. Concentration error bars are estimated from the reproducibility of the pipet. Fluorescence values are averaged over five positions on three independently prepared slides. Values shown are corrected for background fluorescence measured from BSA-glass plus PBS but not for fluorescence arising from bulk-dissolved molecules in the evanescent illumination. Fluorescence error bars are standard error in the mean for the 15 point averages. The observation area is 2.45 μm^2 and the incident laser power is 0.02 mW/μm^2.

Fluorescence vs. Bulk Concentration

To interpret a TIR/FCS autocorrelation function, one must know the average fraction β of surface binding sites that remain free (Eq. 4) at equilibrium. Fig. 5 indicates that R-IgG surface concentration increases linearly with applied bulk concentration. For a single binding process, this means that the number of R-IgG molecules on the surface (neglecting those in the evanescent wave) is much less than the number of sites for nonspecific binding, such that $\beta \approx 1$. If a multiplicity of binding processes occur, some types of sites might be saturated and others not. However, the saturated site components would be a minor contribution to the total fluorescence, as no plateaus are evident in Fig. 5. Thus, we assume β = 1. The simplest interpretation of the positive abscissa intercept is that 0.03 mg/ml (i.e., 0.006 mg) of R-IgG adsorbs to the sample chamber for applied concentrations ~0.1 mg/ml.

Immunoglobin Autocorrelation Function

Surface concentration fluctuations in R-IgG on BSA-glass are seen through the microscope eyepiece as randomly flashing (spatially and temporally) fluorescence fluctuations. These fluorescence fluctuations, observed by the photomultiplier over ~5 μm^2 through a 40X, 1.3 numerical aperture, oil-immersion objective, are autocorrelated with reasonable statistical accuracy in 5–45 min. Fig. 6 displays the autocorrelation function of 0.023 ± 0.0005 mg/ml R-IgG adsorbing to BSA-glass and observed over 4.4 μm^2. Data composited from sample times equal to 0.03, 0.1, 0.5, and 5 ms are shown. $G(\tau)$ has been corrected (as described above) for slow drifts in fluorescence intensity (≤10%) and for background intensity (measured for BSA-quartz plus PBS, ≤10% of the total signal). To substract correlations from systematic fluctuations (i.e., equipment vibrations, etc.), a similarly corrected autocorrelation function taken from the same sample with observation area 300 μm^2 [$G(\tau) \leq$ 0.0005 for all τ] has been subtracted. No difference in $G(\tau)$ decay time is observed for 0.5 and 5 ms data over threefold increase in concentration, observation areas as small as 0.4 μm^2, or a threefold decrease in power. Autocorrelation of the fluorescence fluctuations from a slide coated with dil and mounted identically to the R-IgG samples gives rise to a $G(0)$ values <5% of that shown in Fig. 6.

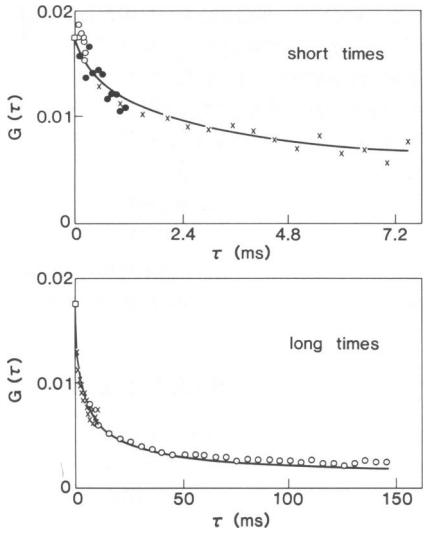

FIGURE 6 Autocorrelation of R-IgG adsorbing to BSA-glass. Data points are composited from autocorrelation functions accumulated with sample times 0.03 ms (○), 0.1 ms(●), 0.5 ms (×) and 5 ms (○), and have been corrected for slow drifts in fluorescence intensity, for background intensity, and for systematic fluctuations, as described in the text. The R-IgG bulk concentration is 0.023 ± 0.005 mg/ml, and the observation area is (2.1 μm)^2. The laser power is 0.02 mW/μm^2 for the 5 and 0.5 ms data, a factor of 3 higher for the 0.1 ms data and another factor of 3 higher for the 0.03 ms data. The line represents a function of the form of Eq. 8 with R_B = (5.3 ms)$^{-1}$; R_R = (0.4 ms)$^{-1}$, and $G(0)$ = 0.0176 as discussed in the text. The deviation of the theoretical curve from the data points at very early times represents the correction described in the text for R-IgG dissolved in the bulk solution within the evanescent wave.

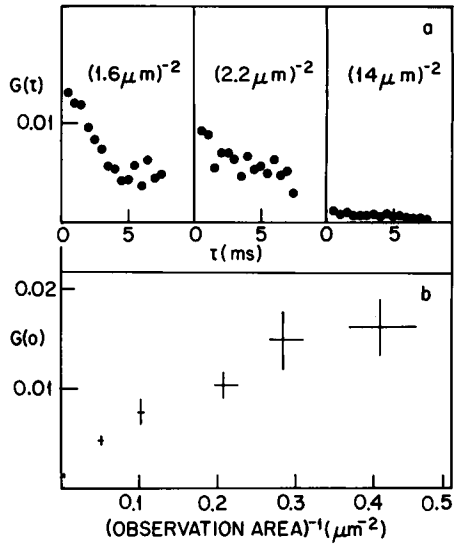

FIGURE 7 R-IgG zero value vs. observation area. $G(0)$ increases for smaller observation areas for a given surface concentration. (*a*) $G(\tau)$ at short times for three observation area sizes. The concentration of R-IgG is 0.015 mg/ml (R/I = 0.38), and the laser intensity is 0.02 mW/μm^2 (for small observation areas) or 0.007 mW/μm^2 (for observation area 0.005 μm^{-2}). Each autocorrelation function was accumulated in 5 min, and has been corrected (as described earlier) for slow drifts in fluorescence intensity and for background intensity. (*b*) $G(0)$ (extrapolated from curves like those in *a*) vs. the reciprocal of the observation are. Each point is the average of four values; error bars for $G(0)$ are standard error in the mean, and error bars for inverse observation area are estimated from the image plane aperture accuracy.

Zero Value vs. Observation Area

The magnitude of $G(\tau)$ should be inversely proportional to the number of fluorescent molecules in the observation area (Eq. 9). For a given concentration of R-IgG in the bulk, and thus a given concentration on the surface, $G(0)$ should be inversely proportional to the size of the observation area. Fig. 7 demonstrates that such a relationship holds, except for the smallest area. The effective size of the smallest observation area is probably underestimated because it is close to the limit of optical resolution. The value approached by $G(0)$ at infinite observation area (the ordinate intercept) is the size of fluctuations in the system due to sources of noise other than molecular number fluctuations and is ~0.001.

R-IgG Data Analysis

As previously described (Thompson et al., 1981), the surface binding process is reaction limited if 1/2-decay time ($\equiv\tau_e$) of $G(\tau)$ is $>> \tau_B = (\beta\langle C\rangle/\langle A\rangle)^2/D_A$; the process is bulk-diffusion limited if $\tau_e \approx \tau_B$. For $\langle C\rangle$ = 9.7 ± 0.8 fluorophores/μm^2, $\langle A\rangle$ = 15.0 ± 3.2 fluorophores/μm^3 (from the value of $G(0)$ and the fluorescence calibration experiments described above), β = 1, and D_A = 5 × 10^{-7} cm^2/s, τ_B equals 8.4 ± 2.7 ms. This means that the adsorption process giving rise to the function in Fig. 6 (which appears to have a characteristic time in the several millisecond range) is probably limited by the rate of R-IgG diffusion in solution.

The time course of $G(\tau)$ does not change from that in Fig. 6 for observation areas as small as 0.4 μm^2, thereby indicating that surface diffusion does not appreciably affect $G(\tau)$. For surface diffusion to be apparent, a typical R-IgG molecule must diffuse across the observation area in the time it remains bound. For a bulk-diffusion limited $G(\tau)$, the average time a molecule remains bound to the surface is less than ~10 ms. Thus, for the smallest observation area, surface diffusion would not be observed unless it had a coefficient D_C of at least 4 × 10^{-7} cm^2/s (which is, coincidentally, approximately equal to the bulk diffusion coefficient).

Given that $G(\tau)$ is either at or near the bulk-diffusion limit, and that it does not depend on the size of the observation area, $G(\tau)$ should be of the form of Eq. 8. We have compared the values of Eq. 8 for several combinations of R_R and R_B to the experimental values of $G(\tau)$. Only times >1 ms are included in the analysis, in that experimental values at earlier times might be determined partially by bulk diffusion through the evanescent illumination. For the same reason, $G(0)$ is not taken equal to the experimental value (0.019), but to the calculated value (0.0176), as discussed earlier. For each pair of R_R and R_B, we calculate the chi-squared deviation summed over all the points in $G(\tau)$; the relative weight assigned to each point in

the sum is taken to be proportional to the slope of the theoretical function at that point. The minimum chi-squared is for R_B = (5.3 ms)$^{-1}$, and R_R much larger, beyond the range of the data. This means that $G(\tau)$ represents an adsorption/desorption process that is nearly bulk-diffusion limited. Nevertheless, lower and upper limits can be established for R_R (the chemical desorption rate, Eq. 7). Curve fitting of the data indicates a lower limit of ~(0.5 ms)$^{-1}$. Consideration of the adsorption residency time on the surface relative to the bulk-diffusion time for traversing the evanescent wave that is necessary to yield the known fraction (0.87 ± 0.09) of surface-bound illuminated molecules indicates an upper limit of ~(0.1 ms)$^{-1}$ for R_R.

The equilibrium constant is determined by $\langle C \rangle$, $\langle A \rangle$, and $\langle B \rangle$, and is equal to 0.65 μm/$\langle B \rangle$. For $\langle B \rangle$ = 10^4 sites/μm^2 (an estimate), K would equal 3.9 × 10^4 M^{-1}, corresponding to an adsorption binding energy at room temperature of ~6 kcal/mol. Given the equilibrium constant and the allowable range for R_R ($=k_2$ for $\beta \approx 1$; see Eq. 7), we can calculate that k_1 is between 0.8 × 10^8 and 4 × 10^8 M^{-1}s^{-1}.

Comparison of R-IgG and R-insulin on BSA-glass

Fig. 8 shows autocorrelation functions obtained under similar conditions on BSA-glass for an applied R-IgG concentration of 0.033 mg/ml and an applied R-insulin concentration of <0.002 mg/ml. The incident laser power is a factor of 3 or more dimmer than for the data in Fig. 6. In that the insulin concentration in solution is not precisely calibrated, no analysis in terms of the previously developed theory is applied to the curves in Fig. 8. Instead, we compare the average times for which R-IgG and R-insulin autocorrelation functions have decayed to the midpoint value between that at 5 and 300 ms. We find this time to be 30 ± 1 ms for R-IgG and 40 ± 1 ms for R-insulin.

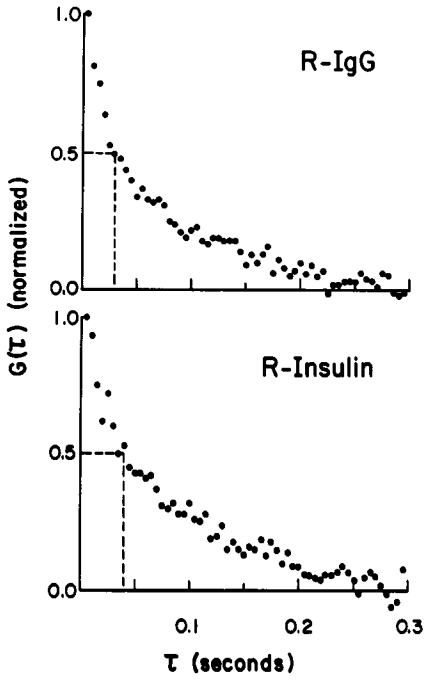

FIGURE 8 Typical autocorrelation functions of R-IgG and R-insulin on BSA-glass. $G(\tau)$ is normalized so that the value at 5 ms is 1 and the average value at 300 ms is 0. The time for half decay between 5 and 300 ms is somewhat longer for R-insulin than for R-IgG.

SPECIFIC BINDING RESULTS

We have measured the fluorescence of bivalent monomer and univalent F_{ab} fragment R-MOPC and RTEPC adsorbing at equilibrium to DNP-BSA-glass and BSA-glass. The sample preparation is identical to that described for R-IgG plus BSA-glass, except that fluorescence is excited with laser intensity 0.01 μW/μm^2 and collected from a large observation area (~500 μm^2) with a 50X, 1.00 numerical aperture objective (E. Leitz Inc.). Fluorescence measurements are taken at several positions on several independently prepared slides and averaged. Thus, for the slide containing R-MOPC on DNP-BSA-glass, the fraction of measured fluorescence α arising from R-MOPC specifically bound to immobilized DNP groups is

$$\alpha \equiv 1 - \frac{F[\text{BSA + R-MOPC}] \cdot F(\text{DNP-BSA + R-TEPC})}{F[\text{DNP-BSA + R-MOPC}] \cdot F[\text{BSA + R-TEPC}]}, \quad (15)$$

where F[] denotes fluorescence intensity measured on a particular combination of antibody and surface.

For an applied bivalent R-MOPC concentration of 0.05 ± 0.005 mg/ml, we find α = 0.78 ± 0.04. The specific binding fraction α decreases with increasing bulk concentration; at 0.2 mg/ml, $\alpha \approx 0.3$. The fraction of fluorescence arising from reversibly bound antibody is measured by flashing the excitation light to photobleach surface-bound fluorescent-labeled antibodies, and monitoring subsequent fluorescence recovery as reversibly bound photobleached molecules exchange with unbleached ones from the solution. (This technique is called TIR/FPR; see Burghardt and Axelrod, 1981; Thompson et al., 1981.) The fraction of the fluorescence that is reversible after 5 min, determined by TIR/FPR, for bivalent R-MOPC on DNP-BSA-glass, is 0.07 ± 0.03. The fraction that is reversibly bound for the other combinations of rhodamine-labeled bivalent myeloma proteins on BSA surfaces is R-MOPC on BSA-glass, 0.44 ± 0.08; R-TEPC on DNP-BSA-glass, 0.20 ± 0.04; R-TEPC on BSA-glass, 0.52 ± 0.08. Although these fractional recoveries may reflect a small amount of surface-bound cross-linked protein induced by the light flash (Sheetz and Koppel, 1979; Dubbelman et al., 1978; Lanni et al., 1981), the reversible fraction for bivalent R-MOPC on DNP-BSA-glass is observed to be consistently lower than for other samples, over many preparations of antibody and hapten-coated surface. In light of these reversibility

results, the 22% of the fluorescence arising from nonspecifically bound bivalent R-MOPC accounts for (0.22 ± 0.04) (0.44 ± 0.08) (0.20 ± 0.04)/(0.52 ± 0.08) = 0.04 ± 0.01 of the 0.07 ± 0.03 fractional recovery. This leaves 0.03 ± 0.03 reversibily and specifically bound bivalent R-MOPC. Thus, the kinetic binding rates of the the bivalent antibody are not easily measured by TIR/FCS.

One would expect that R-MOPC univalent hapten-binding fragments would bind overall less strongly to a hapten-coated surface. We have measured α for R-MOPC F_{ab} on DNP-BSA-glass to be 0.2 ± 0.3. Thus, for this surface, the equilibrium constant and/or the number of binding sites is greater for nonspecific than for specific binding. The protein fluorescence quenching experiments (Fig. 4) demonstrate that the F_{ab} are active for DNP in solution. In addition, the bivalent monomer experiments demonstrate that the DNP groups on the surface are accessible to the antibody. Thus, a reasonable conclusion is that the F_{ab} in fact reversibly bind to the DNP-BSA, but in the company of many nonspecifically bound F_{ab}.

DISCUSSION

The experiments on the nonspecific adsorption of R-IgG and R-insulin to BSA-glass demonstrate the capability of TIR/FCS to measure, in equilibrium, reversible binding of a fluorescent-labeled protein to a surface. They also demonstrate the control experiments necessary to interpret a TIR/FCS autocorrelation function. In contrast to the techniques of stopped flow and temperature, pressure, and concentration jump, TIR/FCS is performed with no extrinsic perturbation from chemical equilibrium and requires no spectroscopic or thermodynamic change between the dissociated and complexed states of the reaction. In addition, TIR/FCS can determine the absolute number of illuminated fluorescent molecules independent of the efficiencies of fluorescence emission and detection. As a surface chemistry technique, TIR/FCS should be particularly useful where both surface adsorption and surface diffusion occur.

The kinetics measured for nonspecific adsorption of R-IgG and R-insulin on BSA-glass are more rapid than those usually observed in protein adsorption experiments. The nonspecific binding of serum albumin to bare fused silica exhibits a multiplicity of binding rates (Burghardt and Axelrod, 1981). One might also expect to observe a multiplicity of rates in these R-IgG adsorption experiments. Thus, the R_B and R_R values generated by the data analysis of the autocorrelation function in Fig. 6 would reflect average values. In reality, multiple binding types each have separate R_B values (determined by the equilibrium constants) and R_R values (determined by the off-rate k_2 and the degree of surface site saturation). If each process acts on independent surface binding sites, $G(\tau)$ is the sum of curves in the form of Eq. 8, weighted according to the fraction of the surface-bound molecules that are binding with each type of process. If the binding processes compete for the same surface binding sites, $G(\tau)$ is even more complicated.

Most light-induced artifacts would cause a change in the decay rate $G(\tau)$ with a change in incident laser intensity. This is not observed for R-IgG on BSA-glass. Still, some consideration must be given to the potential existence of such phenomena. One possibility is that fluorescence fluctuations arise from R-IgG molecules that bind either irreversibly or with slowly reversible binding to sites on the surface and subsequently become photobleached by the incident light. This is unlikely, in that the characteristic time of photobleaching for protein-conjugated rhodamine at the intensities used in the experiments is considerably longer than the characteristic decay time of $G(\tau)$.

Another artifact that might occur is light-induced cross-linking of the rhodamine-labeled immunoglobulin. Cross-linking of membrane proteins upon illumination has been observed with fluorescein-concanavalin A–labeled erythrocytes (Sheetz and Koppel, 1979), fluorescein-labeled erythrocyte ghosts, and baby-hamster kidney cells in the presence of protoporphyrin (Dubbelman et al., 1978). In addition, an increase with illumination in polymerization of 5-iodoacetamide fluorescein-labeled actin has been observed (Lanni et al., 1981). For these R-IgG TIR/FCS experiments, a slow increase in measured fluorescence is occasionally observed, which might correspond to light-induced aggregation of protein on the surface. The effect is present only for R/I values or illumination intensities that are higher than those of the presented data.

Another possible artifact is local heating of the solution near the interface by excited rhodamine molecules and resultant altered reaction kinetics. For a typical experiment illuminating fluorescent-labeled cell surface components, the local temperature rise during illumination has been calculated to be <0.03°C (Axelrod, 1977). The laser intensity in this calculation was a factor of 50 larger than that of our evanescent wave, and the fluorophore concentration was a factor of 500 greater than our rhodamine density. It is therefore unlikely that local heating alters the measured R-IgG binding kinetics.

Specific binding of univalent anti-DNP to DNP-BSA-glass is accompanied under equilibrium conditions by a large amount of nonspecific binding to the surface. Specific binding of bivalent anti-DNP to the surface is also accompanied by nonspecific binding, but the nonspecifically bound antibody represents a smaller fraction of the total bound antibody (at least for low concentrations). Although TIR/FCS is clearly successful in measuring rapid adsorption/desorption reaction rates at equilibrium, measurement of specific rates requires a surface to which the solubilized molecules do not indiscriminately adsorb.

Our anti-DNP experiments are quite different from

those in which particular cell-surface components are identified by incubating with fluorescent-labeled antibodies or other fluorescent-labeled molecular markers (Taylor and Wang, 1980). In cell-surface labeling techniques, the cell is incubated for a short while with a high concentration of antibody and then washed several times, so that only irreversibly bound antibody remains. The experiments described in this paper suggest that during labeling the cell surface may be coated with an appreciable amount of nonspecifically adsorbed antibody. This may also occur for biological cells in vivo, since antibody concentration in the blood can be as high as 50 mg/ml (Eisen, 1974). Thus, rapidly reversible nonspecific binding between soluble proteins (e.g., antibodies or hormones) and cell surfaces (containing, for example, antigens or hormone receptors), or between two soluble proteins, may accompany or precede specific binding. Adam and Delbrück (1968) and Berg and Purcell (1977) have postulated that such nonspecific binding accompanied by surface diffusion might even perform a biological function by enhancing the overall reaction rate with specific receptor molecules.

The authors thank Thomas Burghardt, who built much of the TIR optical apparatus, and wrote versions of the nonlinear curve-fitting programs; Doran Smith, who designed the photomultiplier-to-minicomputer interface; and Anne Maddelena and Latham Claflin who provided purified MOPC 315 protein.

This work was supported by National Institutes of Health grants NS14565 and HL24039.

Received for publication 29 October 1982 and in final form 21 March 1983.

REFERENCES

Adam, G., and M. Delbrück. 1968. Reduction of dimensionality in biological diffusion processes. *In* Structural Chemistry and Molecular Biology. A. Rich and N. Davidson, editors. Freeman Press, San Francisco, 198–215.

Amante, L., A. Ancona, and L. Forni. 1972. The conjugation of immunoglobulins with tetramethylrhodamine-isothiocyanate: a comparison between the amorphous and the crystalline fluorochrome. *J. Immunol. Methods.* 1:289–301.

Aragón, S. R., and R. Pecora. 1976. Fluorescence correlation spectroscopy as a probe of molecular dynamics. *J. Chem. Phys.* 64:1791–1803.

Axelrod, D., D. E. Koppel, J. Schlessinger, E. Elson, and W. W. Webb. 1976. Mobility measurement by analysis of fluorescence photobleaching recovery kinetics. *Biophys. J.* 16:1055–1069.

Axelrod, D. 1977. Cell surface heating during fluorescence photobleaching recovery experiments. *Biophys. J.* 18:129–131.

Axelrod, D. 1979. Carbocyanine dye orientation in red cell membrane studied by microscopic fluorescence polarization. *Biophys. J.* 26:557–573.

Axelrod, D. 1981. Cell-substrate contacts illuminated by total internal reflection fluorescence. *J. Cell. Biol.* 89:141–145.

Axelrod, D., N. L. Thompson, and T. P. Burghardt. 1983. Total internal reflection fluorescence microscopy. *J. Microsc. (Paris).* 129:19–28.

Berg, H. C., and E. M. Purcell. 1977. Physics of chemoreception. *Biophys. J.* 20:193–219.

Borejdo, J. 1979. Motion of myosin fragments during actin-activated ATPase: fluorescence correlation spectroscopy study. *Biopolymers* 18:2807–2820.

Borejdo, J., S. Putnam, and M. F. Morales. 1979. Fluctuations in polarized fluorescence: evidence that muscle cross bridges rotate repetitively during contraction. *Proc. Natl. Acad. Sci. USA.* 76:6346–6350.

Brash, J. L., and D. J. Lyman. 1971. Adsorption of proteins and lipids to nonbiological surfaces. *In* The Chemistry of Biosurfaces. M. Hair, editor. Marcel Dekker, Inc., New York. 177–232.

Burghardt, T. P., and D. Axelrod. 1981. Total internal reflection/fluorescence photobleaching recovery study of serum albumin adsorption dynamics. *Biophys. J.* 33:455–467.

Burghardt, T. P. 1982. Serum protein adsorption: kinetics and conformation studied by total internal reflection fluorescence. Ph.D. Dissertation, University of Michigan.

Burghardt, T. P. 1983. Fluorescence depolarization by anisotropic rotational diffusion of a luminophore and its carrier molecule. *J. Chem. Phys.* In press.

Burghardt, T. P., and D. Axelrod. 1983. A total internal reflection fluorescence study of energy transfer in surface adsorbed and dissolved bovine serum albumin. *Biochemistry.* 22:979–985.

Clark, W. R. 1980. The Experimental Foundations of Modern Immunology. John Wiley & Sons, Inc., New York, 1–372.

Cuatrecasas, P. 1975. Hormone-receptor interaction and the plasma membrane. *In* Cell Membranes: Biochemistry, Cell Biology, and Pathology. G. Weissmann and R. Claiborne, editors. H. P. Publishing Co., Inc., New York. 177–184.

Dragsten, P. R., and W. W. Webb. 1978. Mechanism of the membrane potential sensitivity of the fluorescent membrane probe merocyanine 540. *Biochemistry.* 17:5228–5240.

Dubbelman, T. M. A. R., A. F. P. M. De Goeij, and J. Van Stevenick. 1978. Photodynamic effects of protoprophyrin on human erythrocytes: nature of the crosslinking of membrane proteins. *Biochim. Biophys. Acta.* 511:141–151.

Ehrenberg, M., and R. Rigler. 1976. Fluorescence correlation spectroscopy applied to rotational diffusion of macromolecules. *Q. Rev. Biophys.* 9:69–81.

Eisen, H. N., E. S. Simms, and M. Potter. 1968. Mouse myeloma proteins with antihapten antibody activity. The protein produced by plasma cell tumor MOPC 315. *Biochemistry.* 7:4126–4134.

Eisen, H. N. 1974. Immunology: an introduction to molecular and cellular principles of the immune response. *In* Microbiology, by Davis, Dulbecco, Eisen, Ginsberg, and Wood. Harper and Row, Hagerstown, MD. 352–624.

Elson, E. L., and D. Magde. 1974. Fluorescence correlation spectroscopy. I. Conceptual basis and theory. *Biopolymers.* 13:1–27.

Fahey, P. F., D. E. Koppel, L. S. Barak, D. E. Wolf, E. L. Elson, and W. W. Webb. 1977. Lateral diffusion in planar lipid bilayers. *Science (Wash., D.C.).* 195:305–306.

Fahey, P. F., and W. W. Webb. 1978. Lateral diffusion in phospholipid bilayer membranes and multilamellar liquid crystals. *Biochemistry.* 17:3046–3053.

Giaver, I. 1978. A simple visual surface immunology test. *J. Immunol. Methods.* 24:57–61.

Goetzl, E. J., and H. Metzger. 1970. Affinity labeling of a mouse myeloma protein which binds nitrophenyl ligands. Kinetics of labeling and isolation of a labeled peptide. *Biochemistry.* 9:1267–1278.

Grinnell, F., and M. K. Feld. 1982. Fibronectin adsorption on hydrophilic and hydrophobic surfaces detected by antibody binding and analyzed during cell adhesion in serum-containing medium. *J. Biol. Chem.* 257:4888–4893.

Harrick, N. J. 1967. Internal Reflection Spectroscopy. John Wiley & Sons, Inc., New York, 1–327.

Harrick, N. J., and G. I. Loeb. 1973. Multiple reflection fluorescence spectroscopy. *Anal. Chem.* 45:687–691.

Hirschfeld, T. 1965. Total reflection fluorescence. *Canadian J. Spectrosc.* 10:128.

Hirschfeld, T., M. J. Block, and W. Mueller. 1977. Virometer: an optical instrument for visual observation, measurement and classification of free viruses. *J. Histochem. Cytochem.* 25:719–723.

Horbett, T. A., and P. K. Weathersby. 1981. Adsorption of proteins from plasma to a series of hydrophilic-hydrophobic copolymers. I. Analysis with the *in situ* radiodination technique. *J. Biomed. Mater. Res.* 15:403–423.

Janatova, J., J. K. Fuller, and M. J. Hunter. 1968. The heterogeneity of bovine albumin with respect to sulfhydryl and dimer content. *J. Biol. Chem.* 243:3612–3622.

Kahn, C. R. 1976. Membrane receptors for hormones and neurotransmitters. *J. Cell Biol.* 70:261–286.

Koppel, D. E. 1974. Statistical accuracy in fluorescence correlation spectroscopy. *Phys. Rev. A.* 10:1938–1945.

Koppel, D. E., D. Axelrod, J. Schlessinger, E. L. Elson, and W. W. Webb. 1976. Dynamics of fluorescence marker concentration as a probe of mobility. *Biophys. J.* 16:1315–1329.

Kronick, M. 1974. Sensing of structure-specific binding onto functionalized quartz surfaces using total internal reflection fluorescence. Ph.D. Dissertation, Stanford University, Stanford, CA.

Kronick, M. N., and W. A. Little. 1975. A new immunoassay based on fluorescence excitation by internal reflection spectroscopy. *J. Immunol. Methods.* 8:235–240.

Lahav, J., M. A. Schwartz, and R. O. Hynes. 1982. Analysis of platelet adhesion with a radioactive chemical cross linking reagent: interaction of thrombospondin with fibronectin and collagen. *Cell.* 31:253–262.

Lanni, F., D. L. Taylor, and B. R. Ware. 1981. Fluorescence photobleaching recovery in solutions of labeled actin. *Biophys. J.* 35:351–364.

Lartique, D. J., and S. Yaverbaum. 1976. Enzymes immobilized on glass. *In* Progress in Surface and Membrane Science. D. A. Cadenhead and J. F. Danielli, editors. Academic Press, Inc., New York. 361–402.

Lok, B. K., Y. Cheng, and C. R. Robertson. 1983 *a*. Total internal reflection fluorescence: a technique for examining interactions of macromolecules with solid surfaces. *J. Colloid Interface Sci.* 91:87–103.

Lok, B. K., Y. Cheng, and C. R. Robertson. 1983 *b*. Protein adsorption on crosslinked polydimethylsiloxane using total internal reflection fluorescence. *J. Colloid Interface Sci.* 91:104–116.

Lowry, O. H., N. J. Rosebrough, A. L. Farr, and R. J. Randall. 1951. Protein measurement with the Folin phenol reagent. *J. Biol. Chem.* 193:265–275.

Macritchie, F. 1978. Proteins at interfaces. *Adv. Protein Chem.* 32:283–326.

Magde, D., E. L. Elson, and W. W. Webb. 1974. Fluorescence correlation spectroscopy. II. An experimental realization. *Biopolymers.* 13:29–61.

Magde, D., W. W. Webb, and E. L. Elson. 1978. Fluorescence correlation spectroscopy. III. Uniform translation and laminar flow. *Biopolymers.* 17:361–376.

Mosbach, K., editor. 1976. Immobilized Enzymes. *Methods Enzymol.* Vol. 44. 1–999.

Neumann, A. W., M. A. Moscarello, W. Zingg, O. S. Hum, and S. K. Chang. 1979. Platelet adhesion from human blood to bare and protein-coated polymer surfaces. *J. Polymer Sci. Part D Macromol. Rev.* 66:391–398.

Nicoli, D. F., J. Briggs, and V. B. Elings. 1980. Fluorescence immunoassay based on long time correlations of number fluctuations. *Proc. Natl. Acad. Sci. USA.* 77:4904–4908.

Peterson, N., E. L. Elson, and D. Johnson. 1981. Aggregation measurements on cell surfaces by scanning fluorescence correlation spectroscopy. International Workshop on the Biological Applications of Photobleaching Techniques, Chapel Hill, NC. (Abstr.)

Phillies, G. D. J. 1975. Fluorescence correlation spectroscopy and nonideal solutions. *Biopolymers.* 14:499–508.

Potter, M., and R. Lieberman. 1970. Common individual antigenic determinants in five of eight BALB/c IgA myeloma proteins that bind phosphoryl choline. *J. Exp. Med.* 132:737–751.

Potter, M. 1972. Immunoglobulin-producing tumors and myeloma proteins of mice. *Physiol. Rev.* 52:631–719.

Rigler, R., P. Grasselli, and M. Ehrenberg. 1979. Fluorescence correlation spectroscopy and application to the study of brownian motion of biopolymers. *Physica Scripta.* 19:486–490.

Roberts, H., and B. Hess. 1977. Kinetics of cytochrome c oxidase from yeast embrane facilitate electrostatic binding of cytochrome c showing a specific interaction with cytochrome c oxidase inhibition by ATP. *Biochim. Biophys. Acta.* 462:215–234.

Schecter, Y., J. Schlessinger, S. Jacobs, K. Chang, and P. Cuatrecasas. 1978. Fluorescent labeling of hormone receptors in viable cells; preparation and properties of highly fluorescent derivatives of epidermal growth factor and insulin. *Proc. Natl. Acad. Sci. USA.* 75:2135–2139.

Sheetz, M. P., and D. E. Koppel. 1979. Membrane damage caused by irradiation of fluorescent concanavalin A. *Proc. Natl. Acad. Sci. USA.* 76:3314–3317.

Sorscher, S. M., J. C. Bartholomew, and M. P. Klein. 1980. The use of fluorescence correlation spectroscopy to probe chromatin in the cell nucleus. *Biochim. Biophys. Acta.* 610:28–46.

Sorscher, S. M., and M. P. Klein. 1980. Profile of a focused collimated laser beam near the focal minimum characterized by fluorescence correlation spectroscopy. *Rev. Sci. Instrum.* 51:98-102.

Taylor, D. L., and Y. Wang. 1980. Fluorescently labeled molecules as probes of the structure and function of living cells. *Nature* (*Lond.*). 284:405–410.

Thompson, N. L. 1982 *a*. Immunoglobulin surface binding kinetics studied by total internal reflection/fluorescence correlation spectroscopy. Ph.D. Dissertation, University of Michigan, Ann Arbor, MI.

Thompson, N. L. 1982 *b*. Surface binding rates of nonfluorescent molecules may be obtained by total internal reflection with fluorescence correlation spectroscopy. *Biophys. J.* 38:327–329.

Thompson, N. L., T. P. Burghardt, and D. Axelrod. 1981. Measuring surface dynamics of biomolecules by total internal reflection with photobleaching recovery or correlation spectroscopy. *Biophys. J.* 33:435–454.

Underdown, B. J., E. S. Simms, and H. N. Eisen. 1971. Subunit structure and number of combining sites of the Immunoglobulin A myeloma protein produced by mouse plasmacytoma MOPC 315. *Biochemistry.* 10:4359–4367.

Vroman, L., and A. L. Adams. 1971. Peculiar behavior of blood at solid interfaces. *J. Polym. Sci. Part C.* 34:159–165.

Watkins, R. W., and C. R. Robertson. 1977. A total internal reflection technique for the examination of protein adsorption. *J. Biomed. Mater. Res.* 11:915–938.

Weetal, H. H. 1972. Insolubilized antigens and antibodies. *In* The Chemistry of Biosurfaces. M. L. Hair, editor. Marcel Dekker, Inc., New York. 597–631.

Weis, R. M., K. Balakrishnan, B. A. Smith, and H. M. McConnell. 1982. Stimulation of fluorescence in a small contact region between rat basophil leukemia cells and planar lipid membrane targets by coherent evanescent radiation. *J. Biol. Chem.* 257:6440–6445.

Weissman, M., H. Schindler, and G. Feher. 1976. Determination of molecular weight by fluctuation spectroscopy: applications to DNA. *Proc. Natl. Acad. Sci. USA.* 73:2776–2780.

Whittaker, V. P. 1975. Membranes in synaptic function. *In* Cell Membranes: Biochemistry, Cell Biology and Pathology. G. Weissman and R. Claiborne, editors. H P Publishing Co., Inc., New York. 167–175.

Wong, M., M. E. Bayer, and S. Litwin. 1978. Virus-cell interaction: prediction of the time course of observable effects from virus interaction at cell infection sites, and mechanisms leading to attachment. *FEBS* (*Fed. Eur. Biochem. Soc.*) *Lett.* 95:26–30.

Yardley, J. T., and L. T. Specht. 1976. Orientational relaxation by fluorescence correlation spectroscopy. *Chem. Phys. Lett.* 37:543–546.